Dr. Hugues Brenot
Belgian Institute for Space Aeronomy
Avenue Circulaire n°3
B-1180 BRUSSELS
BELGIUM

February, 28th 2013

Dear Prof. Geraint Vaughan and Dr. Dave Adams,

Authors response to the comments of the referee,

The authors gratefully thank Dr. Dave Adams for his interesting comments which did contribute to improve the manuscript.

Note that in the following text, the comments of the referee are written in dark blue italic and our replies in regular font (in black).

Referee #1 (D. Adams) comments (comments received and published: 7 October 2012):

Summary

The paper "Preliminary signs of the initiation of deep convection by GNSS" by Brenot et al. examines the inclusion of gradients in total zenith delay (ZTD) from a GNSS network over Belgium with the intent of improving near real-time forecasting of convective initiation.
Most GNSS/GPS derived precipitable water vapor studies do not consider the effects of anisotropy and assume azimuthal homogeneity in water vapor fields. This work considers the inclusion of anisotropy when observing water vapor fields (ZTD gradients, in this case). I find this study interesting and definitely worth pursuing and I encourage the authors to do so. However, the paper in its present form needs to be entirely reworked. The paper in its present form lacks quantification and error analysis, contains odd and vague/imprecise language, it requires more explanation

*with respect to the gradient calculation and needs clearer, more enlightening figures. Finally, given that the ultimate motivation of this study is to improve "real-time" forecasting (nowcasting), it is not clear to me why the authors did not compare (in this study, not a future study**)** ZTD and gradients calculated with final orbits to those calculated using real-time predicted orbits. If ZTD estimates degrade radically with use of real-time predicted orbits (I suspect they don't degrade radically), then the point of this study is moot. This question should be addressed in order to assess the viability of the approach used in the study.*

REPLY AUTHORS 1:

We really appreciated your comments and have tried point by point to answer to all your different advices/expectations (see next section about Specific Comments and Technical Issues). References and details have been added to answer to the lack of quantification and error analysis, and to explain more precisely the GPS gradient calculation. Precisions and improvements of the language have been added in the text. For the figure mentioned, we have improved the quality and the clarity. We add also some tests about GNSS observations to quantify the error in calculations (post-processing, influence of orbits quality, and near real-time measurements). We add two figures and a table with our last results of H_2O alerts with operational fast ZTD observations a new section called "GNSS H_2O from fast calculations" (see REPLY AUTHORS 50).

Major Comments to the Authors

Specifically, there is a lack of quantification throughout the paper and the reader has to depend on vaguely expressed qualitative assessments (see below in "Specific Comments and Technical Issues"). For example, there is no assessment of error with respect to decreasing the observation time interval for calculating ZTD or gradients, that is, how much error is introduced in ZTD and gradient values with 15 minute data intervals as opposed to longer intervals (or smaller intervals, e.g., 5 minutes)? This, I suppose, will become even more important when using real time predicted orbits. And, as mentioned above, the error associated with real time predicted orbits needs to be estimated

REPLY AUTHORS 2:

We agree with the fact that more details about the accuracy/variation of different GPS calculations have to be presented in this study (see additional text and results in our answers to the "*Specific Comments and Technical Issues"* and REPLY AUTHORS 50).

Atmospheric instability is mentioned many times throughout the paper, but it is not quantified in any respect. Can you quantify this, for example, with CAPE or with some other measure of instability?

REPLY AUTHORS 3:

We agree also with the fact that some precisions about the indication of the instability have to be added in this study. CAPE and CIN from the radiosounding of Brussels (Uccle) have been added in the text, as well as the estimations of these parameters from Numerical Weather Prediction models (ECMWF and ALADIN). Some details about the regional NWP model ALADIN have been added. The modification of the text section 2 (p. 20353-20354) and the additional Figures are the following:

From the afternoon of the 28th to the evening of the 29th of June 2005, a continuous period of precipitation was observed over the main part of Belgium (as seen Fig. 1). The meteorological situation for this period was the following.

At 00:00 UTC the 29th of June 2005, the isobaric analysis (at 500 hPa and 850 hPa) indicated that a warm and humid air mass was advected from the north of France to Belgium in the lower tropospheric layers. This advection was characterised by a wet bulb pseudo-potential maximum temperature field associated with a ridge of high pressure over Belgium (see Fig. 2.9 and 2.12 of Neméghaire and Brenot, 2010, available on http://h2o.oma.be/RMIB_num59_oct2010.pdf). The surface analysis indicated a complex low pressure area over Belgium and the north of France. It confirmed the advection of mild and humid air mass in the lower tropospheric levels down to the surface. At the surface, this air mass was characterised by high dew point temperatures which increased rather homogeneously up to about 16° to 18°C over these areas. The dew point depression (difference between temperature and dew point temperature at the surface), was small and did not exceed 3°C (see Fig. 2.10 of Neméghaire and Brenot, 2010). The analysis (at 00:00 UTC) of the Convective Available Potential Energy (CAPE) and the Convective Inhibition (CIN) fields from the European Centre for Medium-Range Weather Forecasts (ECMWF with a 30-km resolution) showed CAPE values mostly between 1000 and 2000 J/kg over the North of France while CIN values had locally negative values of about 500 J/kg. Note that a CAPE amplitude 2 or 3 times larger than the associated CIN one indicates a potential instability of the air mass (in our case at 00:00 UTC over the north of France). Nevertheless the 29th at 00:00 UTC, the air remained more stable over Belgium with small CAPE values.

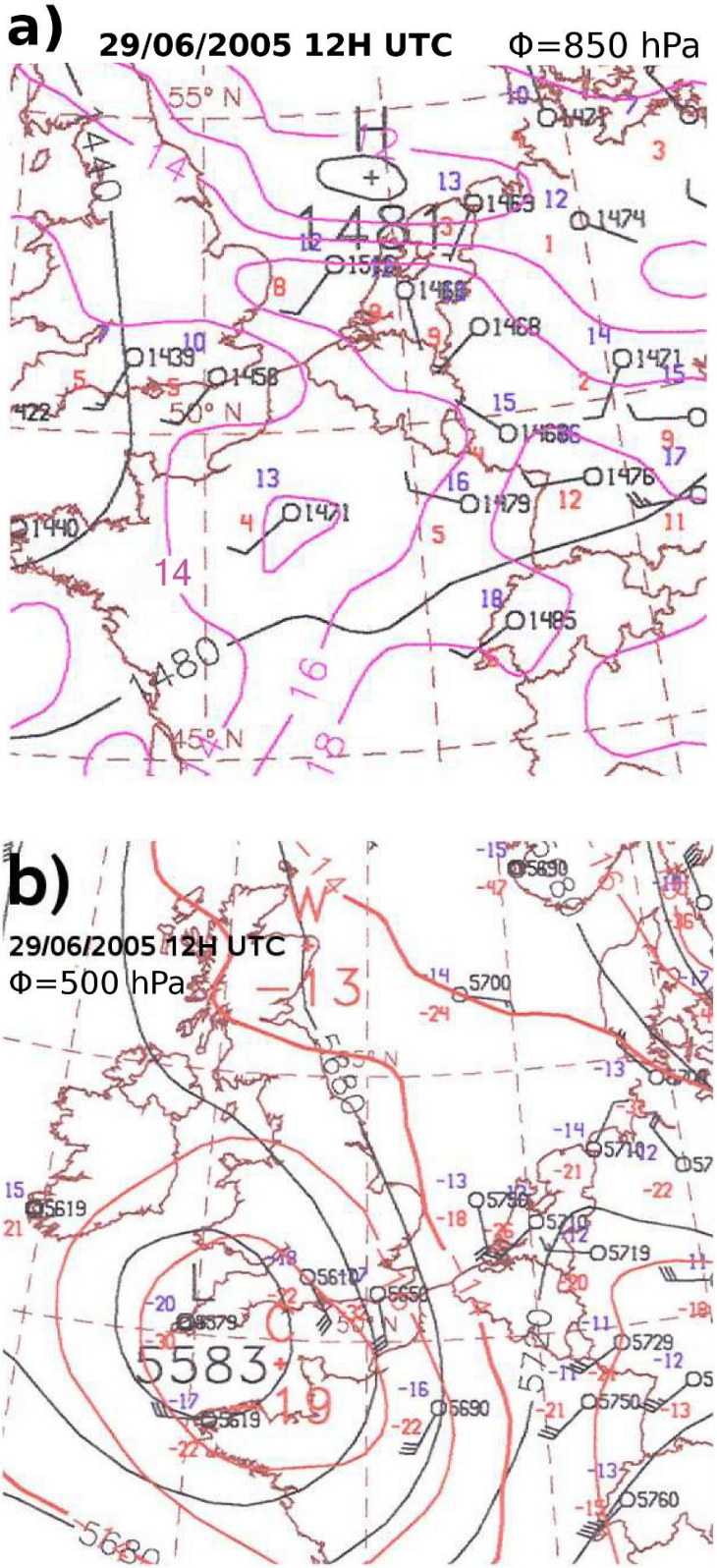

Figure 2: Isobaric analysis a) at 850 hPa, b) at 500 hPa over Western Europe derived from ECMWF background and radiosoundings observations (2005/06/29). The black contours are the geopotential heights. The magenta contours represent the wet bulb pseudo-potential temperature. The observed radiosounding data are pointed on the chart (temperatures in blue, dew point temperatures in red, wind flags and geopotential heights in black).

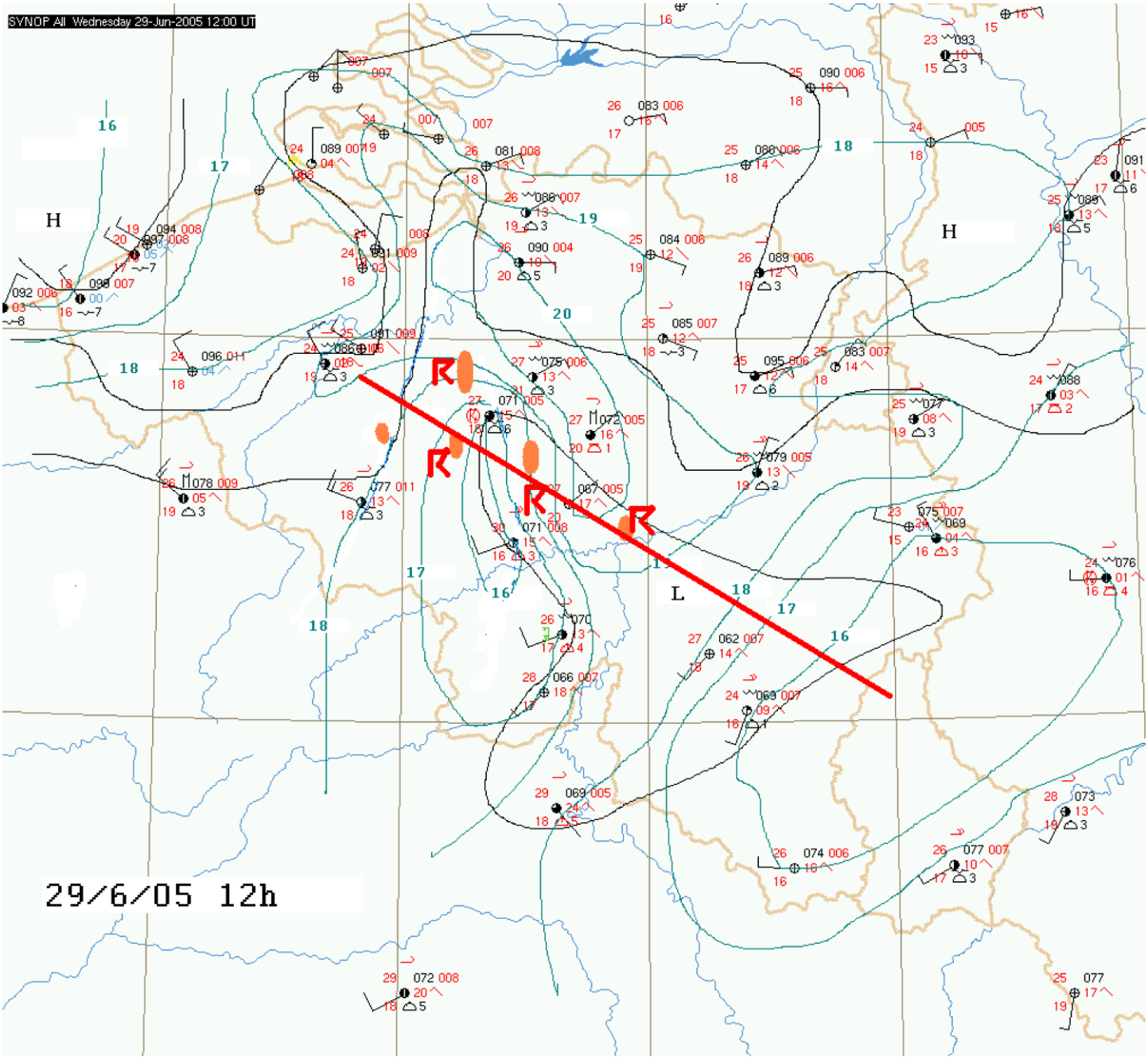

Figure 3: Meso-scale surface analysis based only on observations. Plot of the major line of convergence is shown in red, radar precipitation in orange, thunderstorms detected by SAFIR in R-shape red symbol, contours of the dew point temperature in green, and contours of the mean sea level pressure in black. The synoptic observations are pointed on the chart (temperature and dew point in red, wind flag and the mean sea level pressure in black).

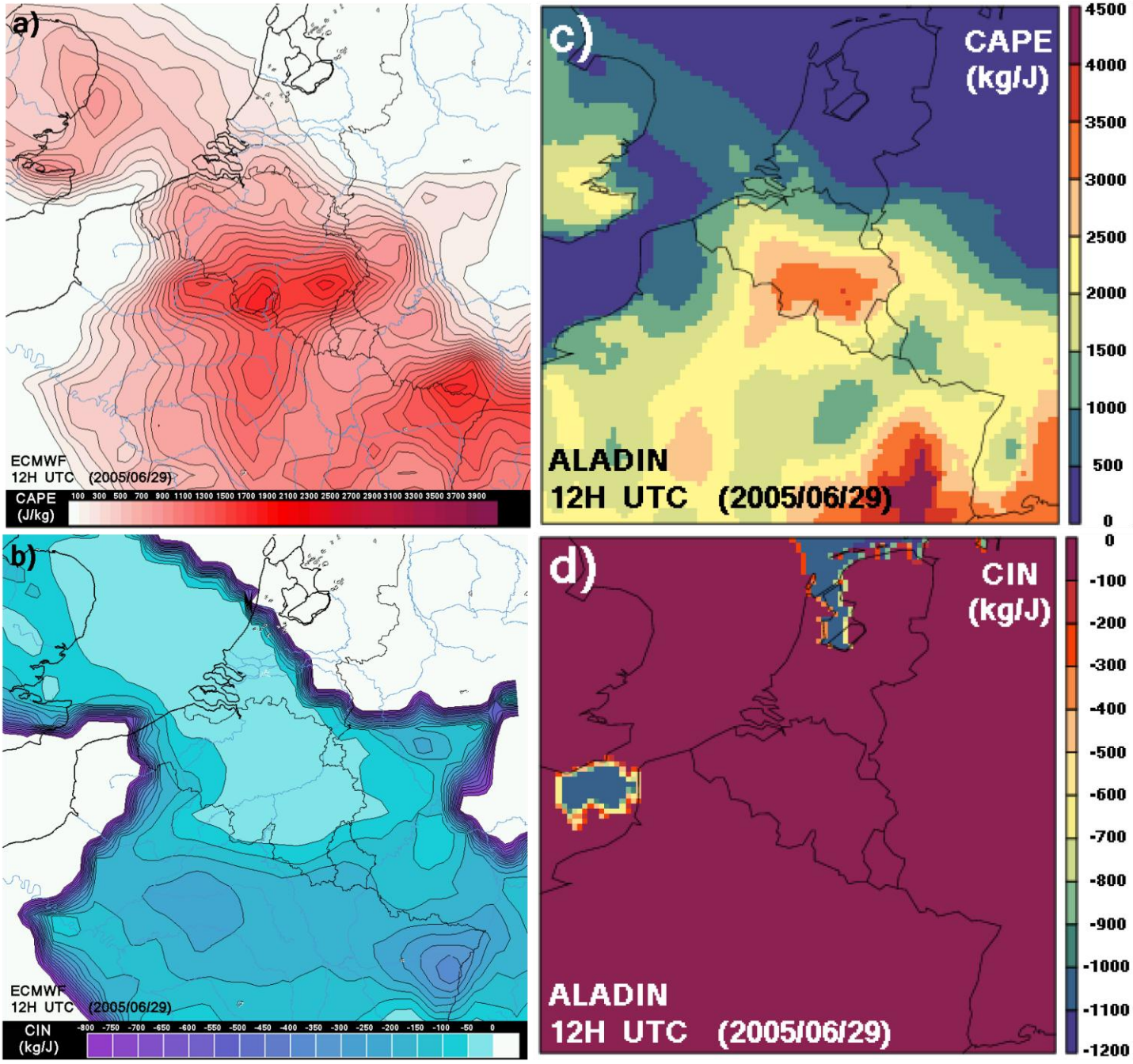

Figure 4: Estimations of a) CAPE and b) CIN from ECMWF model at 12H UTC (2005/06/29). ECMWF model started at 00H UTC (2005/0629). Estimations of c) CAPE and d) CIN from the analysis of ALADIN regional model at 12H UTC (2005/06/29).

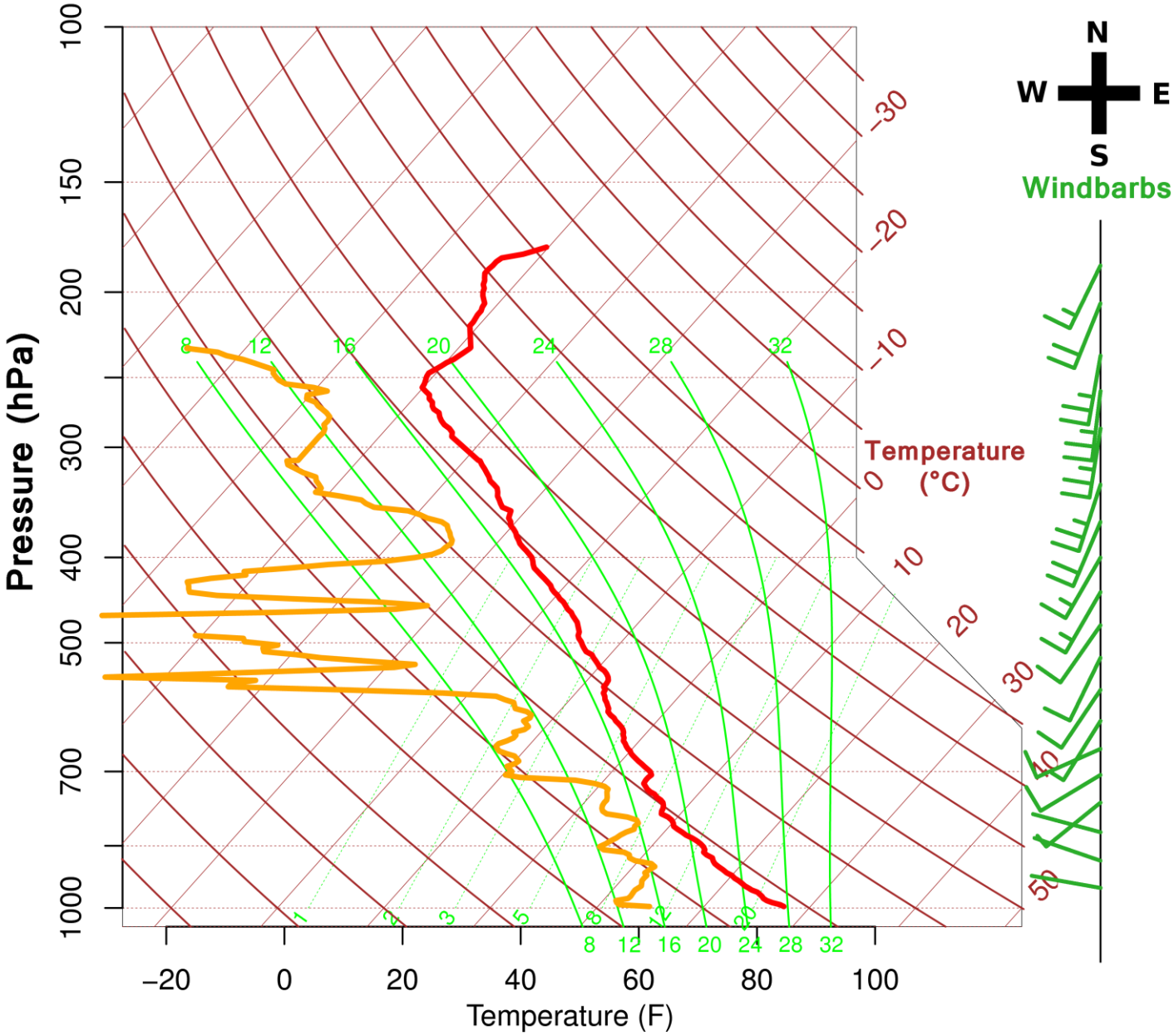

Figure 5: Skew (T - ln P) diagram of the radiosounding measurements at Uccle the 29th of June 2005 at 12:00 UTC (Brussels). The state curve is in red, the dew point curve in yellow, the wet bulb pseudo-potential temperature in green, and the dry adiabatic in brown. The windbarbs are presented on the left in dark green.

At noon the 29th of June, the upper-air isobaric analysis shown Fig. 2b indicated that the ridge of high pressure was gradually giving way to an upper cold air advection associated to a low pressure (L) moving from the northwest of France and the Channel towards Belgium. In the lower troposphere, a "tongue" of rather warm and humid air still remained with wet bulb pseudo-potential temperatures of about 16°C at 850 hPa (see Fig. 2a). We observed a complex low pressure area characterised by several centres which tended to deepen slightly over Belgium

during the afternoon. The warm and humid air mass which has been advected over Belgium the previous night was at this time stagnating. At the surface, this air mass was traced by the analysis of the dew point temperatures (between 16 and 18°C) and a larger dew point depression influenced by the diurnal warming. These higher surface temperature associated to a more inhomogeneous dew point distribution indicated a significant convective mixing at least close to the surface. Using the Belgian synoptic network (pressure and surface winds), lines of convergences have been identified during this event. These were associated with a low pressure trough as shown at 12:00 UTC (2010/06/29) Fig. 3. For this period, using ECMWF model at 12H (initialised at 00H), the CAPE field (see Fig 4a) took significant values (from 1000 to 1600 J/kg), but very low CIN amplitudes (from -50 to -150 J/kg) were shown (see Fig 4b). It indicated a large (static) instability in these areas which remained significant in the afternoon up to at least 18:00 UTC and moved slowly northeastwards. The CAPE and CIN fields computed with our regional limited area model (ALADIN model with a 7-km resolution in 2005; see www.cnrm.meteo.fr/aladin for more details) confirmed the instability detected by ECMWF for the same period, with higher CAPE and lower CIN values obtained over Belgium (see the analysis at 12H UTC Fig. 4cd).

The advection identified by the upper-air and surface analyses (Fig. 2 and 3) has been confirmed by the radiosounding of Uccle (Brussels, Belgium); see the skew (T - ln P) diagram Fig. 5 at 12:00 UTC (2005/06/29) which showed warm and rather moist air in the lower tropospheric layers (with high dew point temperatures) and drier air above 700 hPa (with low dew points). The synoptic station of Uccle was in the area of the convergence line shown in Fig.3, where warm and moist lower air was converging. An increase of the wind which is backing up to the jet stream level (up to 60 knots between 250 to 300 hPa; see the windbarbs presented at the P-level every 10 observations in Fig. 5) was measured by the radiosounding with a CAPE of 868 J/kg and a CIN of -1.05 J/kg (at 12:00 UTC). Note that for this location (Brussels), a CAPE of 1200 J/kg and a CIN of -37 J/kg was obtained from ECMWF model, and a CAPE of 1671 J/kg and a CIN of 0 J/kg from ALADIN model. The signature of warm and moist air in the lower tropospheric area was characterised by high wet bulb pseudo-potential temperatures. At 12:00 UTC, The dry air above 700 hPa indicated a decreasing wet bulb pseudo-potential temperature with altitude which can contribute to a stronger convective instability.

To summarize, between 10:00 and 16:00 UTC on the 29th of June, the surface analysis and the CAPE/CIN fields from the radiosounding at 12:00 (Uccle) and models (ALADIN and ECMWF) indicated a convective episode over Belgium. In the neighbourhood of identified lines of convergence, several clusters of convective cells were developing in a short time (see hourly radar precipitation Fig. 1). Several convective cells were observed by the SEVIRI instrument on

METEOSAT (InfraRed channel). Thick cumuli form clouds with high vertical extensions and cold tops were associated with these cells (see Fig. 6). In the morning of the 29th, clusters of convective cells were distinct with a spatial extension of about 10 km. But finally clusters were stretched by the diffluent air flow in the mid-troposphere and high altitude air currents, as shown on the isobaric analysis at 500 hPa (see Fig. 2b). This diffluent air flow pattern was associated to the low pressure centred over the Channel. A significant variation of the wind speed and its direction following the altitude (indicated by the vertical shear of the wind), affected and increased the vertical development and asymmetric shape of the clusters. The SEVIRI composite visible image (Fig. 7) showed the development of several thick cloud cell, with a signature of cloud stretching and vertical development (indicated by the plume in light blue colour). The shapes of these cloud cells were strongly related to the wind shear in the troposphere along the convergence line (see Fig. 3). The intensification of convective activity induced a complex meso-scale convective system. Gradually this system covered the major part of Belgium resulting in heavy precipitation (up to about 100 mm/day) and thunderstorms. In the north-west of 185 the country, the convective activity was limited (see Fig. 1). Neméghaire and Brenot (2010) gave a more precise description of this meteorological event.

The prediction of rainfall from this complex convective system, using ECMWF and the regional forecast from ALADIN, using data from the Belgian synoptic network and the near real-time meteorological observations (radar, SAFIR, METEOSAT), was not so helpful at this time for the nowcasting.

Note that 4 news authors has been added to this study:

P. De Meutter[3,2], A. Deckmyn[2], A. Delcoo[2], L. Frappez[2]

H. Brenot[1], J. Neméghaire[2], L. Delobbe[2], N. Clerbaux[2], P. De Meutter[3,2], A. Deckmyn[2], A. Delcoo[2], L. Frappez[2], and M. Van Roozendael[1]

[1]Belgian Institute for Space Aeronomie, Avenue Circulaire 3 B-1180 Brussels (Belgium)
[2]Royal Meteorological Institute of Belgium, Avenue Circulaire 3 B-1180 Brussels (Belgium)
[3]Astronomical Observatory, University of Gent, Krijgslaan 281 S9 B-9000 Gent (Belgium)

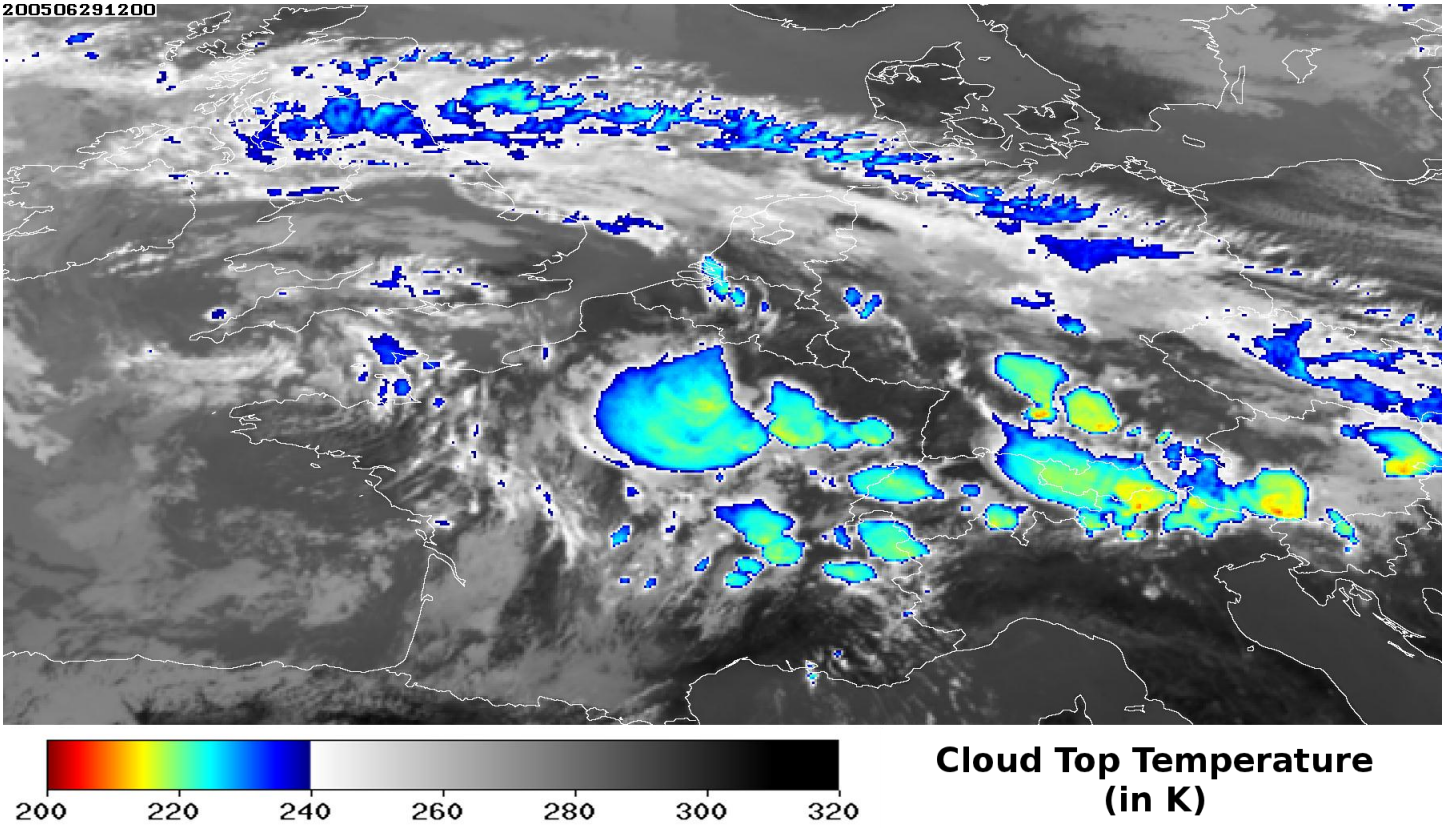

Figure 6: SEVIRI images of the cloud top temperature of the IR channel (2005/06/29 at 12:00 UTC).

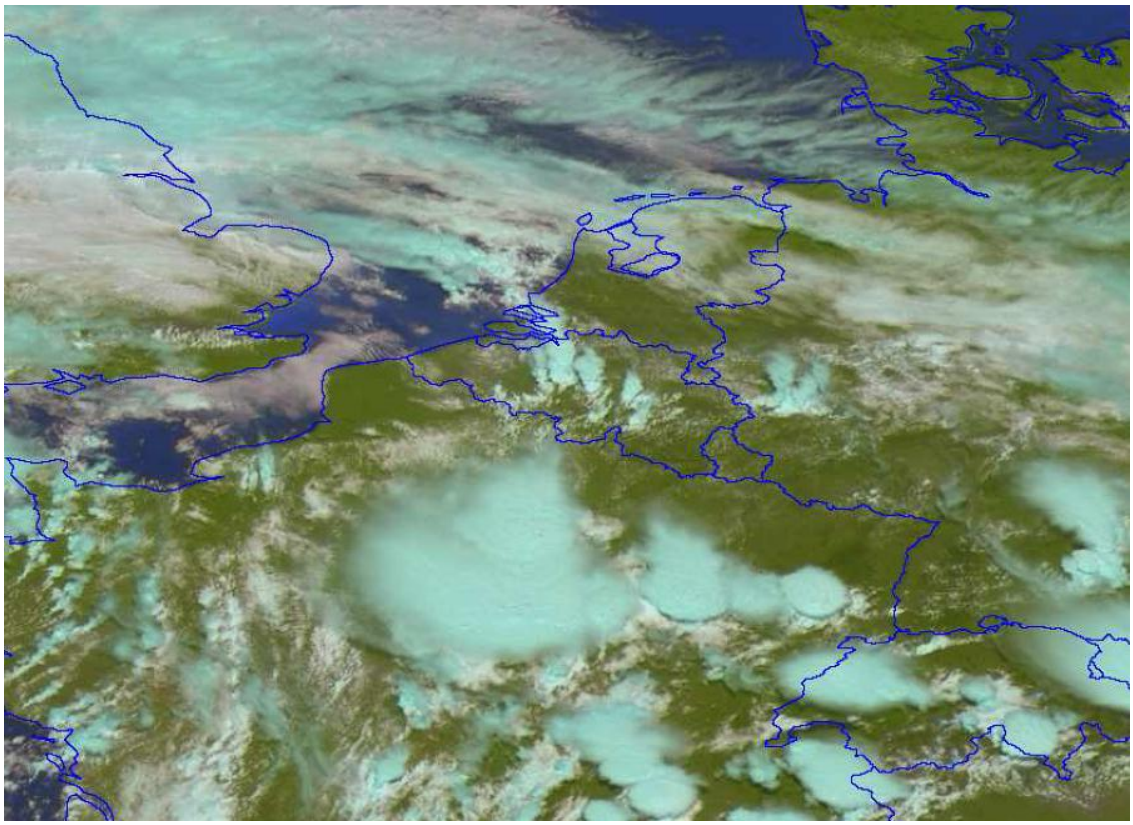

Figure 7: Natural colour composite image of SEVIRI visible channels at 0.6m, 0.8m and 1.6m (2005/06/29 at 12:00 UTC). For the cloud, a blue colour indicates that the top of the cloud is composed of ice crystals while the white indicate liquid water droplets.

A figure of the Belgium dense network of GPS stations has been added.

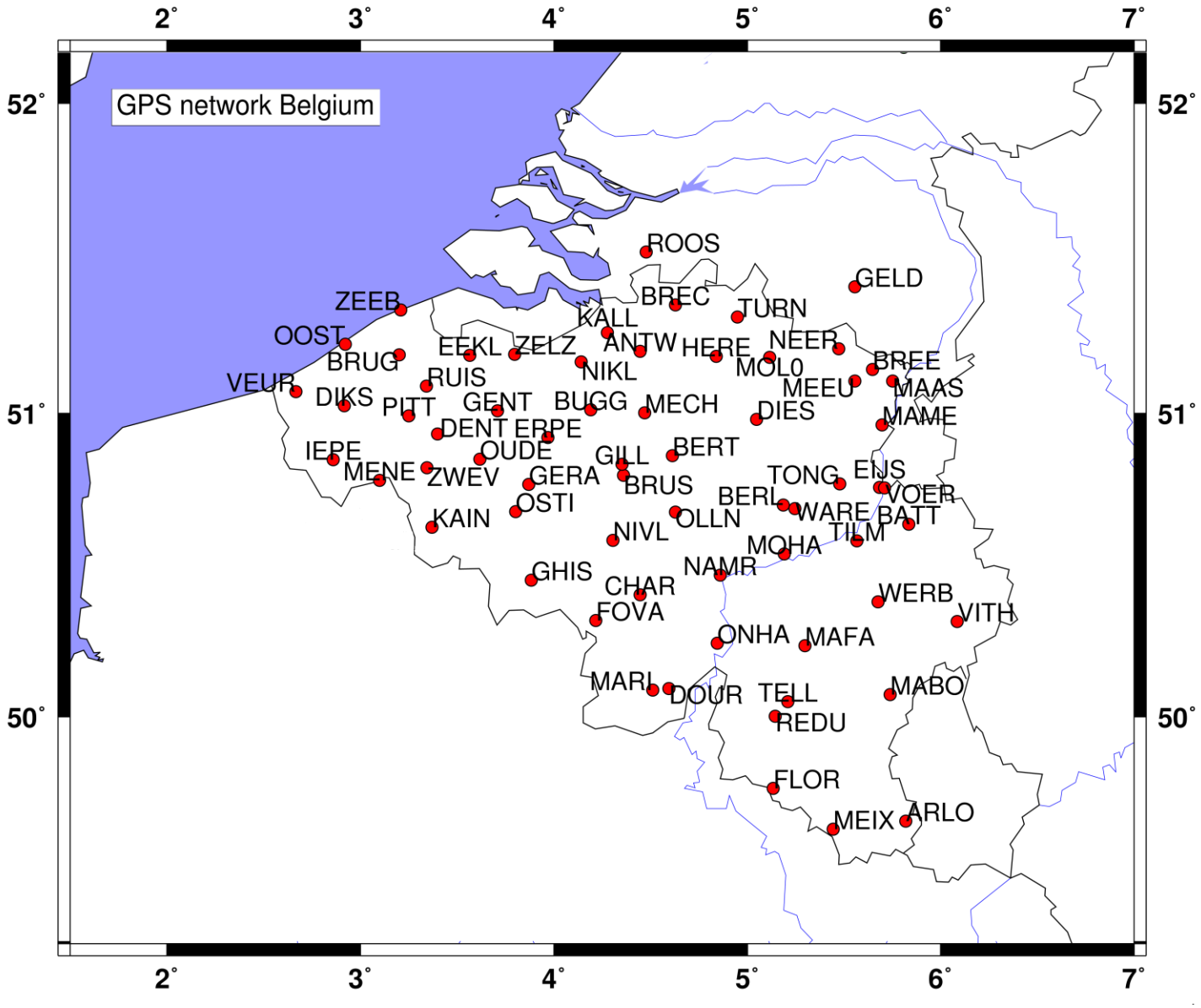

Figure 8: Belgian dense network of GPS stations.

Or, can you quantify the observed gradients in terms of meteorological variables (e.g., temperature, dew point, etc.) so that the reader can better assess the meteorological conditions of your case study.

REPLY AUTHORS 4:

We think that the local heterogeneity of the water vapour density field observed by horizontal GNSS gradients (local anisotropy) defined by two components (NS and EW) is the only meteorological variable. Note that the variations of Zenith Total Delay of the troposphere (ZTD) and gradients of delays are related to the variations of the Integrated Water Vapour content (IWV). Possibly, in another study which uses GNSS tomography and temperature profiles (from

RS, model or others techniques of observations), dew point temperature or other meteorological parameters could be envisaged.

REPLY AUTHORS 5 (modification of line 4-7 p. 20356):
GNSS gradients, described by two components NS and EW, estimate the local anisotropic contribution of slant path delay around a GNSS antenna (which is related to the local water vapour anisotropy, see Gradinarsky 2002); GAMIT normalised this contribution at 10° of elevation (centimetric values of NS and EW components; up to few ten centimetres). Note that 6 mm of delays is equivalent to 1 $kg.m^{-2}$ ~ 1 mm of precipitable water.

This would give the reader a feel for the strength of the water vapor/temperature gradients along which deep convection is developing (independent of the GNSS-derived ZTD gradients).

REPLY AUTHORS 6:
To help the feeling of the reader to better understand the meteorological situation and how the amplitude of gradient and their location of water vapour structure can be related to the initiation of deep convection, more details about the surface analysis and the indicators of the instability (CAPE/CIN) during this event have been added in this study (see next section and REPLY AUTHORS 3, 13, 14, 15, 16 and 17).

Throughout the paper, there is a great deal of odd, imprecise and unclear uses of language that makes the paper difficult to read.

REPLY AUTHORS 7:
OK we agree with that and try to do our best to improve the imprecise language.

Some of the terminology and the variables used are not really common in the atmospheric sciences literature, for example, "digital counts (DC)" and "Neutrosphere".

REPLY AUTHORS 8:
See modifications in the next section.

There are many uses of the word "humidity" that need to be specified; that is, relative, absolute, integral measures, etc.

REPLY AUTHORS 9:

We agree that our terminology about the humidity is too vague and often inappropriate. We avoid as much as possible this term in this study, using generally water vapour content or field.

We modify the next lines:

p. 20352, lines 4 and 7
p. 20353, lines 4, 9, 10 and 12
p. 20354, lines 20 and 22
p. 20355, line 20
p. 20356, lines 17, 19 and 22
p. 20357, lines 8, 13 and 15
p. 20358, lines 5 and 25
p. 20359, lines 15 and 18
p. 20360, lines 14, 15, 18, 20, 21, 23 and 26
p. 20361, lines 1, 5, 9, 10, 12, 15, 19, 22, 26 and 28
p. 20362, lines 4, 20 and 24
p. 20363, lines 21, 22 and 25
p. 20364, lines 18 and 23
p. 20365, line 5

Furthermore, many statements, such as, "But finally clusters were stretched by high altitude air currents (associated with a depression coming from France) and by the impact of the vertical shear of the wind" do not convey much information and are confusing. More examples will be cited below in the section "Specific Comments and Technical Issues".

REPLY AUTHORS 10 (correction of p. 20354, line 1-2):

See REPLY AUTHORS 3.

REPLY AUTHORS 11 (correction the caption of Fig. 2, p. 20372):

Meso-scale surface analysis based only on observations. Plot of a line of convergence is shown in red, radar precipitation in orange, thunderstorms detected by SAFIR in R-shape red symbol, contours of the dew point temperature in green, and contours of the mean sea level pressure in black. The synoptic observations are pointed on the chart (temperature and dew point in red, wind flag and the mean sea level pressure in black).

REPLY AUTHORS 12:

Sorry for that, but we forget the legend of this CTT image (Fig. 3). The legend has been added on the image and the caption has been modified). See Fig. 6 REPLY AUTHORS 3.

Note that "cloud top temperature" has been added to the keywords of the paper.

REPLY AUTHORS 13 (additional text p. 20354, line 4):
See REPLY AUTHORS 3

REPLY AUTHORS 14 (new figures added + text):
See Fig. 2 REPLY AUTHORS 3.

REPLY AUTHORS 15 (correction the text p. 20354, line 9-12):
See REPLY AUTHORS 3.

REPLY AUTHORS 16 (additional text p. 20354, line 12):
See REPLY AUTHORS 3.

REPLY AUTHORS 17 (new Fig.):
See Fig. 7 REPLY AUTHORS 3. There is no colour bar available for this natural colour composite image.

The methodology is not entirely transparent, in particular, with respect to the actual calculation of anisotropy in the ZTD. There is a reference to Chen and Herring (1997) and a few others, but how they exactly apply here is not absolutely clear. There should be a bit more detail given, particularly considering that ground-based GNSS/GPS meteorology comprises a minuscule percentage of ACP articles or that the reader who is more interested in the "prediction of convective initiation" aspect of your study may have limited knowledge of GNSS ground-based meteorology. Some of the references meant to provide more/clearer explanations of the meteorology and/or the gradient calculation are written in French or are not in easily accessible references. This necessitates more explanation directly in the text.

REPLY AUTHORS 18 (modification of the text of section 3.1, p. 20354-20355):
Since 1992 (Bevis et al.), GNSS networks have been used to characterise horizontal water vapour content fields of the troposphere. We have measured ZTD and horizontal gradients of delay with the GAMIT geodetic software (version 10.4, Herring et al., 2010).
To measure such atmospheric observations, a precise knowledge of the positions of all GNSS stations is required. Initially, ZTD and horizontal gradients of delays have been introduced in GNSS calculations to improve the positioning solution (Bar-Sever and Kroger, 1998). The least-square adjustment of ZTD and gradients by GAMIT software in addition to positions increases the precision of positioning solutions. In a primary GAMIT calculation we have estimated precise coordinates for all the local stations (about 70) of the Belgian dense network. Daily sessions of

calculations for a period of 5 days of GNSS phase records have been processed (ZTD estimated every 2 hours, and gradients every 6 hours). An unconstrained daily GAMIT positioning solution has been obtained and converted into a final global solution in the ITRF2000 reference frame (Altamimi et al., 2002) where GLOBK Kalman filter (Herring et al., 1990) has been used and in which the positions of 10 fiducial GPS stations have been constrained. The precision of our positioning solutions obtained with Niell mapping function (1996) is millimetric, which is enough for our meteorological application.

Using the precise positions of stations, a secondary GAMIT calculation has been processed to obtain meteorological observations. Zenith tropospheric delays and horizontal tropospheric gradients (two components, north-south and east-west) are calculated considering reference zenith and gradient variations of $0.02 mh^{-1/2}$ (Herring et al., 2010, Sect. 2.3, 7.3 and 7.4). Tropospheric parameters of the ambiguity free solution have been adjusted with baselines greater than 2000 km. This is a way to un-correlate tropospheric measurements and vertical position estimations in the double difference process (Tregoning et al., 1998). For more details see Brenot et al. (2006).

Finally, ZTD measurements have been produced using a sliding window strategy with 6 sessions of 12 hours of data shifted by 4 hours for daily measurements (see Herring et al. 2010; Chapter 1, Brenot, 2006). A cut-off angle of 10° has been applied. ZTD and gradient observations have been assessed with a time resolution of 15 minutes.

REPLY AUTHORS 19 (modification of the text of section 3.2, p. 20355, line 21-27 and p. 20356, line 1-9):

Ground-based GNSS receivers record the evolution of the phases of the dual frequency GNSS signal (phases L_1 = 1.57542 GHz et L_2 = 1.22760 GHz) emitted by all the satellites. The absolute slant phase delay in direction of a satellite can't directly be measured. The integer number of phase cycle (call the ambiguity) need to be fixed (Bock et al., 1985, 1986; Dong and Bock, 1989; Leick, 1989) to know precisely the slant delays in direction of a satellite. After the ambiguities of the signal in directions of GNSS satellites have been fixed, GAMIT software proceed to a second calculation to estimate ZTD and gradients. The ZTD are obtained considering a priori Zenith Hydrostatic Delays (ZHD) combined with Zenith Wet Delays (ZWD) adjustments established from the phase residuals between model and phase records in directions of satellites (Tregoning and Herring, 2006); see Brenot et al. (2006) for a description of ZHD and ZWD. Simultaneously the GNSS gradients of delays are adjusted considering the phase residuals and a correction of the mapping function (Niell, 1996) with an azimuthal dependency (Chen and Herring, 1997; Herring et

al., 2010, section 7.4). Two components (North-South and East-West) are adjusted (for more details see Davis et al. 1993; Gradinarsky, 2002). Note that the delays of GNSS signals are induced by the ionosphere and the neutral atmosphere. The ionosphere is dispersive for GNSS signals. The use of double difference of a linear combination of L_1 and L_2, so-called ionosphere-free combination (see Spilker, 1980 ; King et al., 1985 ; Brunner and Gu, 1991; Brenot and Warnant, 2008), allows to focus only on the delay induced by the neutral atmosphere.

The (isotropic) first contribution of the reconstruction of the slant delay (1^{st} order of amplitude) is the projection of the ZTD in the direction of the satellite direction. For a station located at the sea level, the ZHD (induced by all the density of the dry and wet troposphere) can be estimated to about 2.2 m. The variation of the ZWD (induced by water vapour) can be from 0.05 m up to 0.5 m. The projection of ZTD at 10° of elevation can be about 14 m (with a contribution of water vapour to the path delay from about 0.3 m to 3 m).

The second (anisotropic) contribution can be obtained using the gradient of delays. This contribution can be up to about 0.2 m at 10° of elevation (2^{nd} order of amplitude). GNSS gradients, described by two components NS and EW, estimate the local anisotropic contribution of slant path delay around a GNSS antenna (which is related to the local water vapour anisotropy, see Gradinarsky 2002); GAMIT normalised this contribution at 10° of elevation (centimetric values of NS and EW components; up to few ten centimetres). Note that 6 mm of delays is equivalent to 1 $kg.m^{-2}$ ~ 1 mm of precipitable water. Contributions of GNSS gradients to slant delays (Chen and Herring, 1997) can be mapped in the zenith direction (Niell ,1996); millimetric values can be observed (up to few centimetres) and will be used in this study.

The figures with images are too small, in particular, 1, 6 and 10 are difficult to interpret.

REPLY AUTHORS 20:

Figure 1 and 10 has been slip to increase their sizes. Figure 6 has been modified (GNSS H_2O alert in full blue lines). The size of figure 6 has been increased in the final version.

Perhaps, Figure 5 could include a "difference" figure between the observed ZTD fields. With regards to the basic science, including anisotropy in ZTD fields appears to be sound.

REPLY AUTHORS 21 (In the following figure you can find the difference of ZTD field Fig5b – Fig5a):

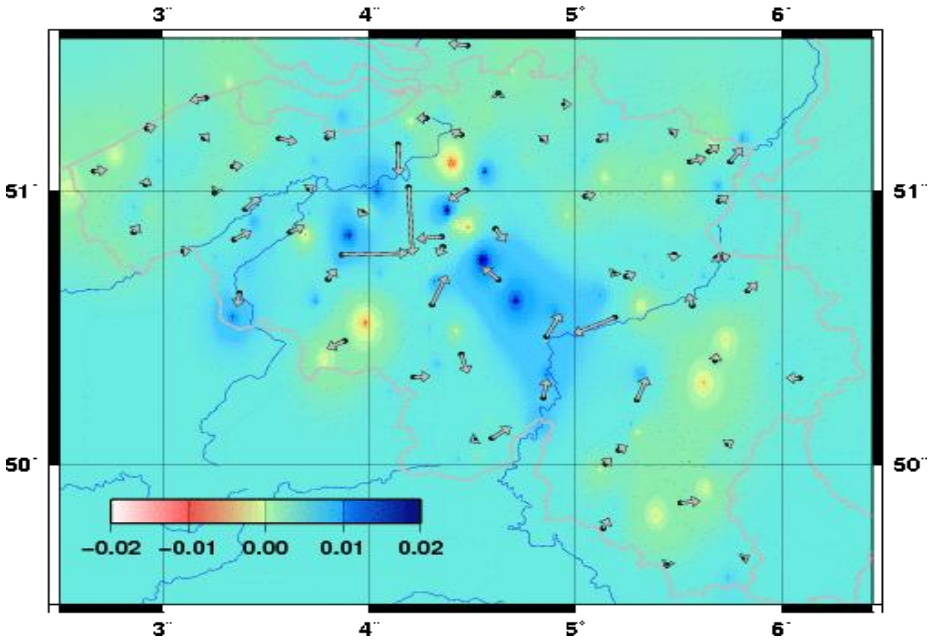

We do not think that this difference corresponds to a noise. The areas where there is more water vapour (in blue) correspond to the new structures of water vapour you can find in Figure 5b. These tropospheric structures are in agreement with the line of convergence identified by our meso-scale analysis and that you can find Fig. 2 (p. 20372). There is no need to add this figure in this study. We really think, there is no doubt that the addition of pseudo-ZTD established from GNSS gradients improves the spatial resolution of the ZTD field observed, which generates more H_2O alerts. You can have a look in the following two figures (on the left, generation of alerts only with the ZTD; on the right, generation of alerts with pseudo-ZTD from gradients):

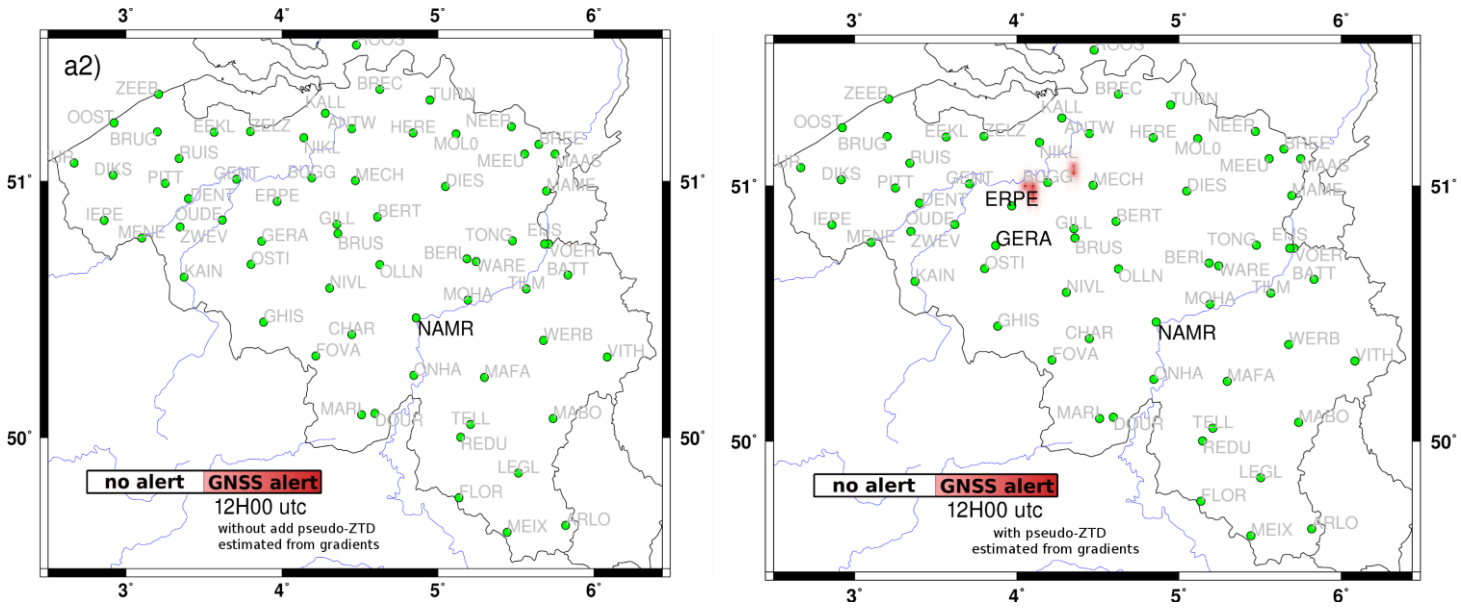

A pixel has a dimension of 3 km x 3.5 km. You can see that there is no alert without the consideration of pseudo-ZTD, and that there is 6 alert pixels considering pseudo-ZTD from gradients. You can see Table 1 that 100% of these alerts has been validated by the radar (altitudes of the highest 38 dBZ radar echoes with values over 5 km).

REPLY AUTHORS 22 (the following text has been added p. 20537, line 8):
The new structures of water vapour identified in Fig 5b are in agreement with the line of convergence shown by our meso-scale analysis (see Fig. 2).

However, I believe a simpler way to relate ZTD measures at individual stations in a network to convective activity exists, without necessarily calculating ZTD gradients. For example, it is not gradients in water vapor, per se, that are responsible for convection or its signal in the data. It is water vapor convergence above the receiver antenna. In this respect, I would suggest just looking at local d (PWV)/dt (d(ZTD)/dt in your case) for each station in the network over the same 15-minute intervals, then, observe the spatial distribution of this variable and how it changes with time over the entire network. Large, rapid increases in PWV (or ZTD), that is, d (PWV)/dt > 0 indicate water vapor convergence over the antenna while rapid decreases in d (PWV)/dt is indicative of precipitation which decreases column water vapor. This behavior is revealed in your Figure 4, without consideration of the gradients. You could attempt to derive your "H20" criteria, based solely on d(ZTD)/dt. The advantage here is that most scientists, researchers, forecasters who work with GNSS meteorological data, have easier access to ZTD (PWV) than to its gradients.
It may be interesting to do two tests for assessing the value of including the ZTD gradients in predicting convective initiation: 1) analyze the evolution of d (ZTD)/dt at each site and its spatial distribution; and 2) assess the evolution of d (ZTD)/dt including the gradients; this way you can determine the contribution of each variable to the prediction of convective initiation.

REPLY AUTHORS 23: I agree that the use of ZTD already provides enough information to generate H_2O alerts. The interest of the GNSS gradients is that we increase the resolution of the ZTD field and the number of warnings generated (see REPLY AUTHORS 21) for location where there is not inevitably a GNSS station.

REPLY AUTHORS 24 (an additional Table 4 has been added in this study):

	Reference processing				**Fast processing**			
Periods	H_2O alerts		Score		H_2O alerts		Score	
2005/06/29 10H45	0	(0)	/	(/)	0	(0)	/	(/)
2005/06/29 10H50	0	(0)	/	(/)	0	(0)	/	(/)
2005/06/29 10H55	0	(0)	/	(/)	0	(0)	/	(/)
2005/06/29 11H00	0	(0)	/	(/)	0	(0)	/	(/)
2005/06/29 11H05	0	(0)	/	(/)	0	(0)	/	(/)
2005/06/29 11H10	0	(0)	/	(/)	0	(0)	/	(/)
2005/06/29 11H15	32	(0)	53.1%	(/)	0	(0)	/	(/)
2005/06/29 11H20	15	(0)	66.7%	(/)	0	(0)	/	(/)
2005/06/29 11H25	0	(0)	/	(/)	0	(0)	/	(/)
2005/06/29 11H30	24	(20)	62.5%	(65.0%)	0	(0)	/	(/)
2005/06/29 11H35	2	(0)	50.0%	(/)	0	(0)	/	(/)
2005/06/29 11H40	3	(0)	0.0%	(/)	36	(0)	30.6%	(/)
2005/06/29 11H45	63	(85)	62.0%	(36.5%)	132	(14)	37.9%	(7.1%)
2005/06/29 11H50	23	(20)	26.1%	(40.0%)	0	(0)	/	(/)
2005/06/29 11H55	0	(0)	/	(/)	0	(0)	/	(/)
2005/06/29 12H00	6	(0)	100.0%	(/)	12	(0)	66.7%	(/)
2005/06/29 12H05	0	(0)	/	(/)	0	(0)	/	(/)
2005/06/29 12H10	8	(0)	100.0%	(/)	0	(0)	/	(/)
2005/06/29 12H15	21	(0)	85.7%	(/)	0	(0)	/	(/)
2005/06/29 12H20	4	(0)	100.0%	(/)	0	(0)	/	(/)
2005/06/29 12H25	23	(1)	87.0%	(100.0%)	23	(9)	78.3%	(44.4%)
2005/06/29 12H30	181	(123)	50.3%	(52.8%)	227	(192)	44.1%	(38.4%)
2005/06/29 12H35	41	(32)	100.0%	(100.0%)	38	(19)	100.0%	(100.0%)
2005/06/29 12H40	13	(0)	100.0%	(/)	7	(0)	100.0%	(/)
2005/06/29 12H45	80	(46)	91.3%	(89.1%)	94	(24)	90.4%	(100.0%)
2005/06/29 12H50	44	(7)	100.0%	(100.0%)	22	(1)	95.5%	(100.0%)
2005/06/29 12H55	28	(8)	42.9%	(12.5%)	9	(0)	0.0%	(/)
2005/06/29 13H00	115	(59)	95.7%	(100.0%)	40	(13)	100.0%	(100.0%)
2005/06/29 13H05	27	(5)	100.0%	(100.0%)	0	(0)	/	(/)
2005/06/29 13H10	13	(0)	100.0%	(/)	0	(0)	/	(/)
2005/06/29 13H15	167	(159)	76.6%	(74.8%)	140	(158)	98.6%	(97.5%)
2005/06/29 13H20	69	(37)	100.0%	(100.0%)	10	(0)	100.0%	(/)
2005/06/29 13H25	1	(0)	100.0%	(/)	10	(0)	100.0%	(/)
2005/06/29 13H30	0	(0)	/	(/)	6	(0)	100.0%	(/)
all this period	1003	(602)	76.4%	(69.6%)	806	(430)	66.5%	(67.4%)

Table 4. Statistics results ($i.e.$ number of alerts and final scores) between 10:45 and 13:30 UTC the 29^{th} of June 2005. The time resolution of GNSS observations is 5 minutes (reference and fast post-processing). The statistics results obtained without the use of pseudo-ZTD established from gradients are presented in brackets.

REPLY AUTHORS 25 (add. text p. 20362, line 15):

Note that statistical results of alerts generated without the use of gradients (see Fig. 5a which shows an example of ZTD field without gradients) are presented in brackets Table 1. The score is also good (67%), which means that our method can also be used without gradients. Nevertheless

the number of alerts is 45% smaller without the use of gradient to improve the ZTD field. This shows the advantage to use gradients to improve the spatial resolution and the number of our GNSS H_2O alerts.

Specific Comments and Technical Issues:

Pg. 20352
Line 20. What do you mean by "mean" meteorological observation?

REPLY AUTHORS 26:
Sorry, we mean "the most used GNSS", text change in the draft.

Line 21. What do you mean by "first order" and "second order" in this context?
Pg. 20353

REPLY AUTHORS 27 (line 21-23):
See REPLY AUTHORS 19. "(1st order)" has been changed to "(strongly related to the water vapour content variation)". "a 2nd order" has been changed to "another".

Line 5. "forerunners" could probably be better expressed as "precursors" or "antecedent conditions"

REPLY AUTHORS 28:
The word forerunners has been changed to precursors in all this study (p. 20352, line 5; p. 20353, line 5; p. 20364, line 18).

Figure 1. What is the color code for? What are the geographical regions? Are they relevant to the issue at hand? This figure is really difficult to see.

REPLY AUTHORS 29:
This figure has been divided in two to increase its size. The colour code (as mentioned in the legend) corresponds to the different geographical region. The interest of this colour code is to show that, for station for example located close to the North-Sea where this is no precipitation recorded by radar, no gradient with strong amplitude has been observed.

Pg. 20354

Figure 3. Put numbers on the values for cloud top temperature.

REPLY AUTHORS 30: See REPLY AUTHORS 12. Sorry for the mistake and thank you for the review, this is CTT which is shown on this figure.

REPLY AUTHORS 31 (add. text p. 20359, line 17-19):
Nevertheless during this event, high GNSS gradients (value up to 0.04 mm) always point in the direction of region where clouds with high top altitudes (> 5 km) have been observed by SEVIRI less than 45 minutes after. For these regions, the CTT are less than 232.5 K (see Fig. 9 and 10)

Line 9 through 13. This is very vague, meteorologically speaking. What do you mean?

REPLY AUTHORS 32:
See modifications of REPLY AUTHORS 12 to 17.

Line 15. Neméghaire and Brenot (2010) is written in French, so it may be of very limited value to the ACP readership.

REPLY AUTHORS 33:
OK, we agree. We decided to leave it because it could still be interesting for a few people.

Line 17. What is ALADIN? Do you have any citations for a description of this model?

REPLY AUTHORS 34:
see REPLY AUTHORS 3 and the modification of the text p. 20354, line 16-19.

Line 21. This is Ground-Based GNSS (GPS) and it essentially gives the column integrated value of water vapor (i.e., precipitable water vapor). Humidity fields is a bit misleading.

REPLY AUTHORS 35:
See modifications in REPLY AUTHORS 9.

Pg. 20355

Line 15. Brenot (2006). If you have this in English, cite that version first.

REPLY AUTHORS 36: Details are presented in Brenot et al. 2006.

Line 21. Typically, the atmosphere is assumed azimuthally homogeneous.

See REPLY AUTHORS 19.

Pg. 20356

Line 10 -15. Again, the behavior in d (ZTD)/dt in the figure is essentially d (PWV)/dt associated with the atmospheric component of the hydrological cycle. Prior to precipitation, d (PWV)/dt is positive, water vapor convergence into the column. After precipitation, column water vapor decreases and d (PWV)/dt decreases. This is not real clear, "high values of gradient components (amplitude 2 times over mean amplitude)"

REPLY AUTHORS 37 (modification of lines 10-15):

High variations of the ZTD field (increase or decrease of 8 mm) and the improvement of its spatial resolution by GNSS gradients is often correlated (score of 63%) with high precipitation (more than 10 mm/hour, see Fig. 1).

Pg. 20357

Line 7. I don't see a huge improvement in the fields in Figure 5. Maybe a difference figure might help emphasize this improvement.

REPLY AUTHORS 38:

See REPLY AUTHORS 21, 24 and modification of Table 1. The horizontal resolution of the water vapour field shown by ZTD is increased. A better characterisation of the water vapour structures is obtained which generates more H_2O alerts.

Line 9 (and throughout the paper). Probably "blobs" is a better word than "bubbles".

REPLY AUTHORS 39:

Bubbles has been replaced by blobs.

Line 23-25. What is of interest is the column of water vapor, not the total tropospheric column. That is, you're looking for the "cone of influence" of water vapor above the receiver. In this case, we use a water vapor scale height

of around 2.5 km and if we assume an average satellite elevation angle of around 30 degrees, then the cone radius would be about 10 km or so.

REPLY AUTHORS 40 (Thanks for this comment. The following text has been added line 25):
Nevertheless, this is the column of water vapour which is of interest for our study. Looking for the cone of influence of water vapour above the receiver, we can use a water vapour scale height of around 2.5 km and then, if we assume an average satellite elevation angle of around 30°, the cone radius is about 10 km.

Pg. 20358
Line 5. ZTD are not "equivalent" to the humidity fields. They are not even equivalent to the PWV fields, but can be used to estimate them.

REPLY AUTHORS 41 (Thanks for this comment, modification of the text line 5):
Using the improvement by horizontal GNSS gradients of the 2D field of ZTD, which can be used to estimate the water vapour field (see Brenot et al., 2006)

Pg. 20359
Line 9 and 21. "Digital Counts" is not something that is used extensively in the atmospheric science literature, use "cloud-top temperature" in Kelvins.

REPLY AUTHORS 42 (modification text p. 20359, line 8-23 and Fig. 9, and new Table):

The second indicator of deep convection that we use is the infrared radiance from the SEVIRI instrument on METEOSAT Second Generation (Chanel 09). The observations used in this study are expressed in Digital Counts (DC). For the 10.8 µm IR channel, the conversion of a radiance in DC (R_{DC}) in a radiance in the International System of units (R_{SI}) is the following:

$$\mathrm{R_{SI}} = \mathrm{R_{DC}} \, . \, gain + offset$$

where the *gain* is 0.205034 and the *offset* -10.456757. The observations of radiance allow us to estimate Cloud Top Temperatures (CTT). This parameter is more commonly used by the meteorologists. The conversion of the radiance in CTT (expressed in Kelvins) is the following:

$$\mathrm{CTT} = \frac{c_2.\nu}{ln\left(1+\frac{c_1\nu^3}{\mathrm{R_{SI}}}\right)}$$

where ν (= 930.659 cm^{-1}) is the central wave number of the 10.8μm-IR band, and c_1=0.00001191066 $mW/(m^2 \cdot sr \cdot cm^{-4})$ and c_2=1.438833 K/cm^{-1} are fixed values.

If the effective radiance (R_{DC}} is less than 200 DC (~ 30.55 $W/m^2/sr/cm^{-1}$), we consider that deep convection took place. A radiance of 200 DC corresponds to a CTT of 232.7423 K (see Table 1).

Radiance R_{DC} (in DC)	Radiance R_{SI} (in $W/m^2/sr/cm^{-1}$)	CTT (in K)
160	22.3487	220.7795
200	30.5500	232.7423
240	38.7514	242.7394
280	46.9528	251.4513
320	55.1541	259.2471
360	63.3555	266.3520

Table 1: Conversion table (channel 09 of SEVIRI) of IR radiance in Digital Counts (R_{DC}) to IR radiance in the International System of units (R_{SI}), and to CTT (in K).

The regions for which SEVIRI identifies deep convection (Fig. 10) are in blue to green and yellow. Over Belgium, the SEVIRI resolution is about 3 km (E-W) x 5 km (N-S). The infrared 10.8 μm channel has been selected because the channel presents the best correlation with the cloud top height. In the weather office of most national meteorological services, this channel is usually used to detect and track convective systems.

The water vapour indicated by GNSS gradients does not always correspond to the location of the convective cells and the clouds with the highest tops identified by SEVIRI. Nevertheless during this event, high GNSS gradients (value up to 0.04 mm) always point in the direction of region where clouds with high top altitudes (> 5 km) have observed by SEVIRI less than 45 minutes after. For these regions, the CTT are less than 232.5 K (see Fig. 9 and 10). We find a good correspondence between low CTT and high gradient amplitudes; 65% of GNSS sites with gradient amplitudes higher than 0.02 m show IR radiances under 220 DC (which corresponds to a CTT of about 238 K). A Pearson negative correlation of 0.36 is obtained between CTT and horizontal GNSS gradient amplitudes.

Line 22. Probably to say a "negative" correlation would be more typical.

REPLY AUTHORS 43:
OK modification of the text line 22.

Pg. 20360
Line 21. Technically speaking, cloud formation is a "sink" or a loss term for PWV, which is what you observe with ZTD. However, convergence may continue to bring water vapor into the column and hence PWV (or ZTD) continues to increase with cloud formation, or even rain, which is a much larger "sink" term.

REPLY AUTHORS 44 (modif. text line 20-22):
An increase of ZTD (and water vapour content) is associated to the development of a deep cloud cell, entertained by the low troposphere flux of water vapour coming from the north and converging into this region. The large vertical extension of this cloud cell was confirmed by IR radiance from SEVIRI showing low cloud top temperature.

Pg. 20362
Line 4. Again, how are you measuring "instability"?

REPLY AUTHORS 45 (see REPLY AUTHORS 3 + modification of the text p. 20362, line 4-6):
Convective cells with low CTT (< 235 K) were detected by SEVIRI on the south side of Belgium, as well as between ROOS and OSTI stations and on the north-east side of Belgium.

Pg. 20363
Line 21. This is a bit unclear. Humidity can vary, but GNSS/GPS is really providing an "integral value" in all cases.

REPLY AUTHORS 46 (modif. text line 21):
This paper shows how to use GNSS gradients to improve the resolution of the ZTD field and the estimation of water vapour.

Pg. 20364

Line 7. The more common variable to consider would be cloud-top temperature.

REPLY AUTHORS 47:

OK see REPLY AUTHORS 42.

Line 17. Again, it is not contrasts or gradients that are precursors to convection, but water vapor convergence, which, of course, can be associated with fronts and gradients in the water vapor fields.

REPLY AUTHORS 48 (modif. text line 16-18):

We have shown the key role of GNSS ZTD combined with horizontal gradients in detecting water vapour blobs and convergences (time and space contrasts between wet and dry regions) which are precursors of deep convection.

Line 26. This should be verified for this study. Am I mistaken, or are the predicted orbits not available for this event period? Or is there something I am missing? If the predicted orbits are available, then how come you didn't attack this issue?

REPLY AUTHORS 50:

Effectively, the predicted orbits are available for this period. We calculate ZTD and gradients with these orbits. There is a very good agreements (no strong degradation) with our reference (post-processing) calculation. We also calculate fast processing ZTD and gradients (more degradation because the sliding windows strategy can't be used in operational calculations).

Section 6 has been split in two subsections (one about validation from post-processed reference calculations and one from fast calculations). Here is the additional text at the end of section 6.1, called "GNSS H_2O alerts from reference post-processing" (with a new Fig.):

To see the impact of the quality of the satellites orbits on ZTD and gradients calculations, we have compared ultra-rapid orbits (IGSU) with our reference calculations with the final orbits (IGSF), both provided by the International GNSS Service (http://igscb.jpl.nasa.gov). We find that these measurements are extremely close (see red and black lines Fig. 16). For a calculation with 35 stations during one week of data, the mean bias and the standard deviation are less than 0.0001 m for ZTD and gradients. An equivalent score for the validation of H_2O alerts is found. In the next session the ultra-rapid orbits will be used to process fast ZTD and gradient measurements.

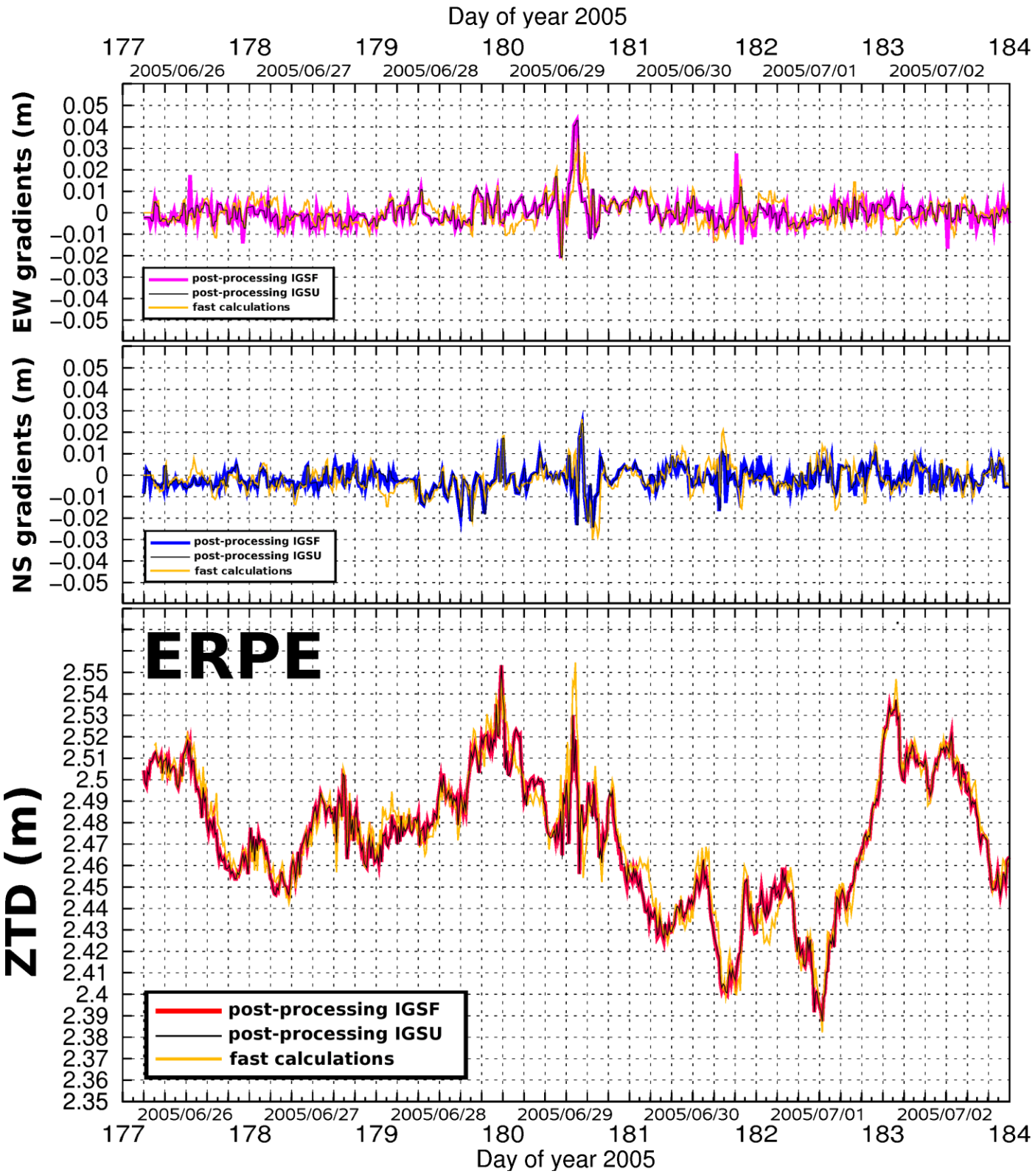

Figure 16: Time-series of ZTD and gradients (from 26 June to 3 July 2005) from post-processed (final orbits IGSF and ultra-rapid orbits IGSU) and from fast calculations.

You can find details about ZTD degradation and the impact on H_2O alerts in a new section 6.2 called "GNSS H_2O alerts from fast calculations":

To estimate ZTD and gradients in an operational way, the use of ultra-rapid orbit is required. In this section, we have used the IGSU orbits. Because the operational use of GNSS observations required a very short time of calculations, we have decided to processed sessions of 6 hours (and not 12 hours like for the post-processing). Six hours is the minimum time to be able to resolve properly the ambiguities of the GNSS signals (see section 3.2). The time of calculations (by least-square adjustment) increases non-linearly in function of the number of stations considered. With 20 stations in a run (10 fiducial stations, 4 long-distance stations, and 6 stations of the Belgian network; see 3.1), this time is about 5 minutes. Twelve process have to be run in the same time to obtain the GNSS measurements of the whole Belgium dense network (70 stations). The fast calculations we present in this section have been done a posteriori. Nevertheless, the quality of these measurements are equivalent to near real-time observations. We can see Fig. 16 that there is a satisfactory agreement between the reference post-processed ZTD and gradients of ERPE station and the fast ones. To complete our ZTD comparison, we processed one week of data, and 7 Belgian stations have been considered: GENT, BUGG, GERA, ERPE, GILL, OUDE, in addition to BRUS which is one on the fiducial stations (see Fig. 8). The mean biases (and standard deviations) between fast and post-processed ZTD and gradients (millimetric zenith estimations) observations are respectively 0.002 (± 0.008) m and 0.001 (± 0.004) m. No sliding window strategy has been considered (which is used usually to avoid the ``side effect'' of the measurements at the beginning and at the end of a session). ZTD and gradients are estimated every 15 minutes in one session. Every 5 minutes a session has been run. The fast ZTD and gradient measurements we considered for a given time are the last ones (at the end) of each session. A very good agreement is obtained between fast and reference post-processed ZTD (less than 10 mm) and gradients (less than 5 mm in the zenith direction; about 25 mm at 10° of elevation). Note that the fast measurements (ZTD and gradients) are generally higher than the reference observations of the post-processing. For your information, the time of calculation for one session of post-processing is 2 hours (giving ZTD and gradient observations for 20 Belgian stations every 15 minutes for a time-window of 4 hours). For fast measurements, this time is about 5 minutes (giving ZTD and gradients for 6 Belgian stations; observations every 15 minutes during 6 hours with only the last period of measurement that we consider).

In Table 4, we present our first statistics results of the validation of H_2O alerts established from fast ZTD and gradient measurements. The period considered is between 10:45 and 13:30 UTC the

29th of June 2005. Reference and fast post-processed measurements results (*i. e.* number of alerts and final scores of the validation using echo top radar and IR radiance from SEVIRI) are presented both with a time resolution of 5 minutes.

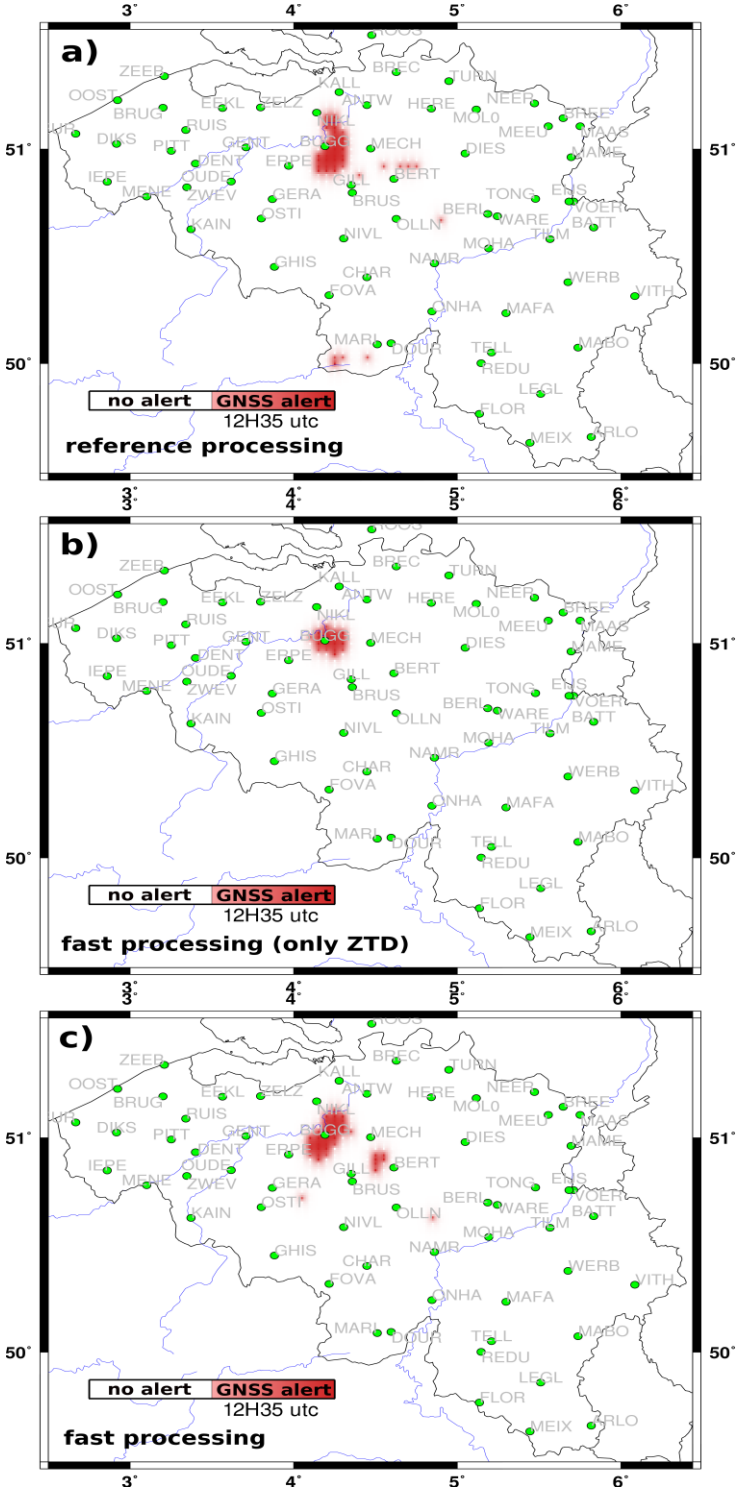

Figure 27: 2D fields of GNSS H_2O alerts (0 or 1) the 29th of June 2005 at 12H35 UTC, a) from reference post-processing measurements (with ZTD and gradients), b) from fast measurements (ZTD only), , b) from fast measurements (with ZTD and gradients).

The number of alerts and the scores shown in brackets Table 4 have been obtained without the use of pseudo-ZTD established from gradients. We see that for both type of calculations, the total number of alerts is 40-45% less without the use of gradients. For post-processed GNSS measurements the score with gradients and pseudo-ZTD is slightly better (69.6% only with ZTD; 76.4% with gradients). We have seen Table 3 that an interpolation of ZTD and gradients measurements from 15 minutes to 5 minutes increases the number of alerts. Logically, a time resolution of 5 minutes shows more alerts (1003) than a time resolution of 15 minutes (see Table 2 with a total number of alerts of 689). For the fast measurements, the score with and without gradient are good and equivalent (respectively 66.5% and 67.4%), which means that our method can also be used without gradient. Nevertheless the number of alerts is 45% smaller without the use of gradients. This shows the advantage to use gradients to improve the spatial resolution and the number of our GNSS H_2O alerts. As an example, Fig. 17b and Fig. 17c show the localisation of the H_2O alerts generated the 29th of June at 12H35 UTC without and with the use of gradients. We can see a good agreement between the alerts generated by reference post-processing and by fast calculations (see Fig. 17ac), which shows the first validation of our method (H_2O alerts) for operational observations.

Note that the abstract and the conclusion have been modified to include the new results with fast post-processing.

Thank you Dave Adams for your very useful comments which really help to improve this paper.

Yours faithfully,

Hugues Brenot